Proceedings of the 17th World Congress
The International Federation of Automatic Control
Seoul, Korea, July 6-11, 2008

Systems Analysis of the Insulin Signaling Pathway ⋆

Eric C. Kwei * **Kevin R. Sanft** ** **Linda R. Petzold** **
Francis J. Doyle, III *

* *Department of Chemical Engineering, University of California, Santa Barbara, CA 93106-5080 USA*
** *Department of Computer Science, University of California, Santa Barbara, CA 93106-5070 USA*

Abstract: Analysis of a detailed mathematical model of the insulin signaling pathway yields a more quantitative understanding of the mechanisms underlying insulin resistance and its subsequent progression to type 2 diabetes. A sensitivity analysis of the model allows optimization of input perturbation as well as state measurement selection for experimental parameter identification. Finally, a stochastic version of the model yields interesting results on the impact of cellular noise on insulin signaling.

Keywords: insulin; signaling pathways; sensitivity analysis; input design; measurement selection; identifiability; stochastic modeling.

1. INTRODUCTION

Overabundant food supply combined with an increasingly sedentary lifestyle, particularly in developed nations, has led to a dramatic increase in the incidence of type 2 diabetes mellitus (T2DM). T2DM has been linked with insulin resistance – a reduced sensitivity of glucose concentration to changes in insulin concentration. Insulin resistance has been hypothesized to be linked to a number of defects in insulin signaling pathways.

One of the functions of insulin is control of cellular glucose uptake in muscle and adipose tissue. This control is carried out through the following signaling cascade (Sesti [2006]). First, insulin binds insulin receptor, which causes receptor autophosphorylation and activation. Activated insulin receptor then phosphorylates insulin receptor substrate-1 (IRS1), which subsequently forms a complex with phosphatidylinositol-3-kinase (PI3K). The IRS1-PI3K complex catalyzes the production of phosphatidylinositol triphosphate (PIP_3) which then interacts allosterically with phosphosinositide-dependent kinase 1 (PDK1). The PIP_3-PDK1 complex phosphorylates protein kinases Akt and protein kinase C (PKCζ). Activated Akt and PKCζ, through an unknown mechanism, trigger glucose transporter (GLUT4) translocation from an internal compartment to the cell membrane. With GLUT4 at the cell membrane, a cell can then uptake glucose from its environment.

This pathway is regulated by the action of a number of other proteins. For example, protein tyrosine phosphatase 1B (PTP1B) dephosphorylates activated insulin receptors and IRS1. In addition, SHIP2 and PTEN (lipid phosphatases) deactivate PIP_3 into $PI(3,4)P_2$ and $PI(4,5)P_2$, respectively.

Notably, two feedback loops modulate the effects of the insulin signaling pathway. Akt can phosphorylate PTP1B, impairing the function of PTP1B as a negative signaling element, resulting in net positive feedback. PKCζ can serine phosphorylate IRS1, which impairs formation of IRS1/PI3K complex, resulting in net negative feedback (Sedaghat et al. [2002]).

With this information, we use the tools of systems biology, specifically sensitivity analysis and stochastic simulation, to model and analyze the insulin signaling pathway. We can then use our analysis of the model to provide recommendations for experimental work, which, in turn, guides model improvement. With sufficient iteration of model improvement and experiment, it may then be possible to explain why certain network perturbations can cause insulin resistance and to identify perturbations that may be useful for treatment (Kitano et al. [2004]).

2. MODEL

Currently, the most mechanistically detailed published model of the insulin signaling pathway was developed by Sedaghat et al. [2002]. Two variations of the model were proposed – one without the feedback mechanisms and one with feedback. Differential equations, derived primarily using mass-action principles, were used to describe the time-varying concentrations of 21 state variables, as illustrated in Fig. 1.

One submodel adds an insulin receptor recycling model to a previously published model of insulin-receptor binding (Wanant and Quon [2000]). Another submodel describes the postreceptor signaling cascade, from phosphorylation of IRS1 to activation of Akt and PKCζ; this submodel also contains the positive and negative feedback loops. The

⋆ This work was supported by the Institute for Collaborative Biotechnologies through grant #DFR3A-8-447850-23002 from the U.S. Army Research Office and by the NSF through IGERT grant #DGE02-2175.

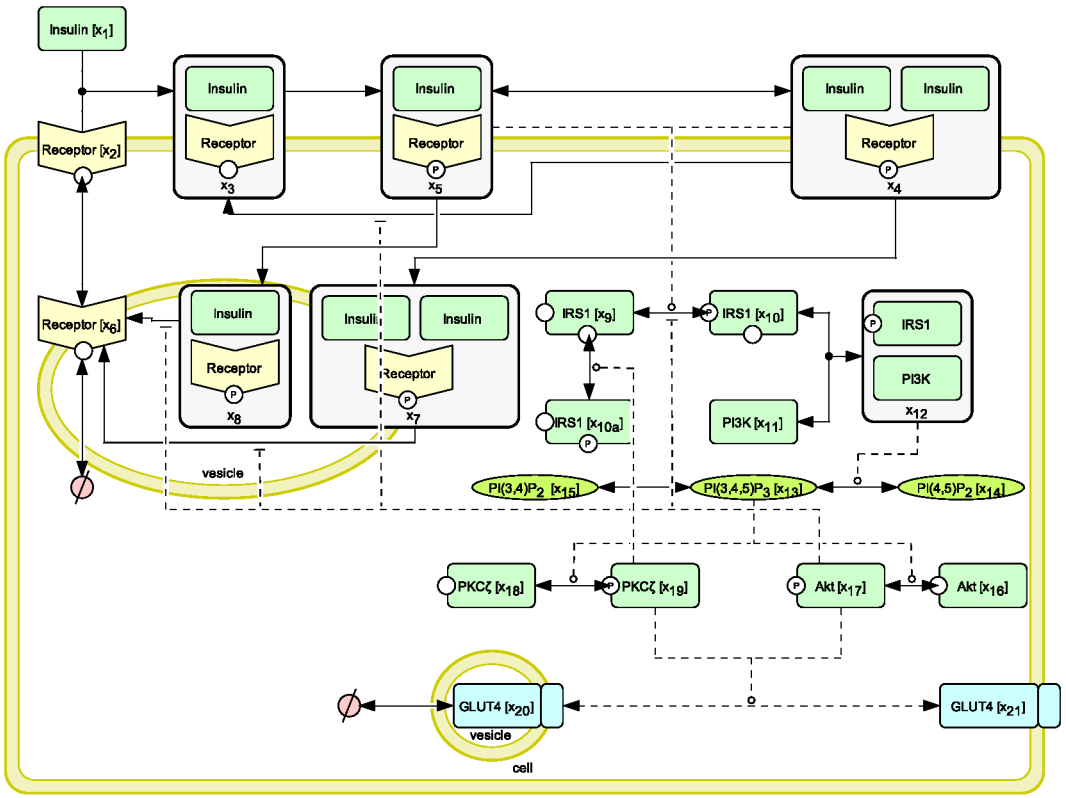

Fig. 1. Model with feedback, adapted from Sedaghat et al. [2002]

final submodel, GLUT4 translocation, describes the effects of Akt and PKCζ on GLUT4 cycling between vesicles and the cell surface (Quon [1994]).

The Sedaghat model, with slight modifications for ease of sensitivity analysis, was compiled in XPP and solved with Runge-Kutta numerical integration over a 60 minute duration (See Appendix A.2). Following Sedaghat, the nominal insulin input concentration was a 15-minute square input, going from 0 M to 10^{-7} M and returning to 0 M.

3. SENSITIVITY ANALYSIS

3.1 Methods

Sensitivity analysis investigates the response of a system to differential changes in parameters. For a system of ordinary differential equations, perturbation of a parameter p_j may cause a change in state x_i; the magnitude of this change is captured by a sensitivity coefficient, S_{ij}.

$$S_{ij}(t) = \frac{dx_i(t)}{dp_j} \tag{1}$$

This sensitivity analysis was conducted using BioSens, a sensitivity analysis tool created by Taylor et al. [2005]. For models in XPP, BioSens uses a centered difference approximation to numerically calculate sensitivity coefficients:

$$S_{ij}(t_k) \approx \frac{x_i(t_k)|_{p_j+\Delta p_j} - x_i(t_k)|_{p_j-\Delta p_j}}{2\Delta p_j} \tag{2}$$

A total of 30 parameters for the model with feedback (28 for the one without) were perturbed by 1% of their nominal values to calculate sensitivities for all states for each time step.

Using these arrays of sensitivities and an estimation of state measurement covariation and assuming that measurements have Gaussian distributions, one can consolidate the information about the system contained by these measurements into the Fisher Information Matrix (FIM). For this application, the FIM is calculated as follows:

$$FIM = \sum_{k=1}^{N_t} S^T(t_k) V^{-1}(t_k) S(t_k) \tag{3}$$

where N_t is the total number of time steps and V, which describes measurement covariance, is a diagonal matrix with elements:

$$V_i = \begin{pmatrix} \sigma_i^2(t_1) & 0 & 0 \\ 0 & \ddots & 0 \\ 0 & 0 & \sigma_i^2(t_k) \end{pmatrix} \tag{4}$$

$$\sigma_{x_i}^2(t_k) = RE_i x_i(t_k) + AE_i$$

In general, when all 21 states were "measured," the relative error for each state (RE) was set to 1 percent, while absolute error (AE) was set to 10^{-7} percent to ensure that V could be inverted. When it was necessary to remove state i from the set of measured states, RE_i was set to 10^7 percent to simulate a highly noisy measurement.

It is very important in a model such as this one (with 21 states and 31 parameters) to be able to estimate parameters as accurately as possible. Following Zak et al. [2003], one can use the FIM to estimate lower bounds on the variance of parameter estimates:

$$\sigma_{p_j}^2 \geq FIM_{jj}^{-1}. \quad (5)$$

A parameter is taken to be identifiable if the 95% confidence interval, $[p_{nominal} - 1.96\sigma_p, p_{nominal} + 1.96\sigma_p]$ does not contain zero. For equivalent numbers of identifiable parameters, one possible optimization is minimizing the average normalized 95% confidence interval $(\frac{1}{N_p}\sum_j 1.96\sigma_{p_j}/p_j)$ over all identifiable parameters, a condition known as A-optimality. Using these formulations of identifiability and optimality, one can then design experiments to maximize the accuracy of parameter estimation.

3.2 Results and analysis

Optimal insulin input selection One strategy to maximize parameter estimation accuracy is to vary insulin input into the system. A number of simple insulin input profiles were analyzed for maximum parameter identification in the model with feedback: 15-minute pulse, 5-minute pulse, step, upward ramp, downward ramp, 1-minute pulse, 0.5-minute impulse, and two 1-minute impulses, spaced 30 minutes apart. The peak values for each insulin input was chosen to be $10^{-7}M$, (as by Sedaghat) to compare similar insulin dosages. The inputs were ranked first by number of identifiable parameters (out of 31), then by A-optimality, with an FIM including all 21 state measurements.

As shown in Table 1, the number of identifiable parameters ranges from 19 to 21 for this variety of insulin inputs, with the best result being the 1-minute pulse. Of the inputs with 21 identifiable parameters, each identifies the same parameters. Therefore, we conclude that input dynamics should have a small but quantifiable effect on the identifiability of model parameters.

An additional point to be made is that while the model without feedback has fewer parameters than the one with (29 to 31), the model with feedback is more readily identifiable. For example, for the 15-minute insulin pulse input, 65% of the parameters can be identified in the model with feedback, compared to 62% for the model without feedback. This also holds true for the insulin step input, with 61% for the model with feedback compared to 52% for the model without. The model with feedback is more identifiable because measurements of early states in the signaling pathway contain information about parameter values for reactions involved in feedback that occur further down the pathway.

Optimal measurement selection Because identifiability was not strongly affected by insulin input dynamics, for ease of calculation, measurement selection was carried out on the 1-minute pulse, which had 21 identifiable parameters. Measurements of as many states as possible were removed from the FIM while maintaining the same number of identified parameters. Then, the FIM's including all permutations of the remaining states were calculated, with the

Input description	Parameters	$\frac{1}{N_p}\sum_j 1.96\sigma_{p_j}/p_j$
1-minute pulse	21	9.84%
5-minute pulse	21	9.98%
0.5-minute pulse	21	11.2%
15-minute pulse	20	6.58%
Ramp up	20	7.61%
Ramp down	20	11.3%
Two 1-minute pulses	19	7.37%
Step	19	15.1%

Table 1. Parameter identification from different input selections, ranked by number of identifiable parameters followed by average width of normalized 95% confidence interval for identifiable parameters

State measurement	Parameters	$\frac{1}{N_p}\sum_j 1.96\sigma_{p_j}/p_j$
$x_2, x_3, ..., x_{21}$	21	9.84%
$x_{15}, x_{17}, x_{19}, x_{20}, x_{21}$	21	11.7%
$x_{15}, x_{17}, x_{19}, x_{20}$	21	16.5%
x_{15}, x_{17}, x_{20}	20	23.0%
x_{15}, x_{17}	14	25.1%
x_{17}	9	46.3%

Table 2. Parameter identification from different measurement selections

results ranked by number of identified parameters and then by A-optimality. The optimal measurement selection for each number of allowed measurements is given in Table 2.

A measurement of only x_{15}, x_{17}, x_{19}, x_{20}, and x_{21} gives 21 identifiable parameters; therefore, nearly all of the parameter information content available is included in these five states, all of which are near the end of the signaling pathway (See Appendix A.1 for more information). As this model for signal transduction is, in general, a signal cascade, the fact that a sparse measurement selection can yield high parameter information content makes sense, as measurements of later states can contain parameter information from reactions involving previous states. Even taking just one measurement (x_{17}) allows one to possibly identify 9 parameters. Although there is no guarantee that the above measurement selections will, in fact, yield the most parameter information for an arbitrary insulin input profile, the conclusion above are likely to be nearly optimal for any input selection.

3.3 Steady-state sensitivity analysis: potential drug targets

Assuming that one could determine the nominal parameter set with any degree of certainty, one might then be able to probe the model for insights concerning the long-term development of insulin resistance. Whereas the case examined by Sedaghat (2002) had a 15-minute square wave input of insulin of amplitude 10^{-7} M, one might be able to simulate a more biologically relevant situation by having a uniform insulin concentration over the duration of the experiment. Due to problems with the mass balances on the components in the model, actual steady-state is not obtained in a realistic time frame and has a non-physical total GLUT4 percentage ($x_{20} + x_{21}$) of greater than 100%. However, by 60 minutes, the slope on surface GLUT4 percentage is fairly small, so scaled sensitivities were calculated at 60 minutes, using the insulin step input

Parameter	Sensitivity
k_{13}	0.673
k_{-13}	(−)0.672
k_9	0.218
k_{-9}	(−)0.218
k_8	0.187
k_{-8}	(−)0.187
k_{11}	0.146
k_{-11}	(−)0.146
k_{-7}	(−)0.138
k_7	0.138

Table 3. List of parameters to which the steady-state surface GLUT4 concentration is most sensitive

Parameter	% change
k_{-12}	696%
k_{12}	695%
k_{10}	230%
k_{-10}	230%
k_9	154%
k_{-9}	154%
k_{-8}	154%
k_8	154%
k_{-11}	(−)27.3%
k_{11}	(−)27.3%

Table 4. List of model parameter sensitivities changed most by removal of feedback mechanisms

case described above with an insulin concentration of 10^{-7} M. This was done for both the model with feedback and without.

Table 3 shows the most sensitive parameters for the model with feedback; all of these parameters represent potential targets for type 2 diabetes therapy. Decreasing values of parameters with negative sensitivities or increasing values of parameters with positive sensitivities would result in higher GLUT4 surface percentages, which, in turn, would lead to higher steady-state rates of glucose transport and lower blood glucose levels.

In addition, one can compare the steady-state performance of the model with feedback mechanisms and the model without (Table 4). The parameter sensitivity increased the most by the removal of feedback, k_{-12}, describes the deactivation of PKCζ; this is indicative of the negative feedback loop involving active PKCζ. As expected from the positive feedback loop involving active Akt, the sensitivity of GLUT4 translocation to k_{-11}, which describes deactivation of Akt, is the one decreased most by the removal of feedback.

4. STOCHASTIC MODELING

Because a number of model species have small copy counts per cell volume (fewer than 10), fluctuations in copy counts may have a profound effect on model behavior (Giri et al. [2004]). As a result, we developed and simulated a stochastic version of Sedaghat's insulin signaling pathway model using Gillespie's stochastic simulation algorithm (SSA), implemented in the StochKit software package (Gillespie [1976]).

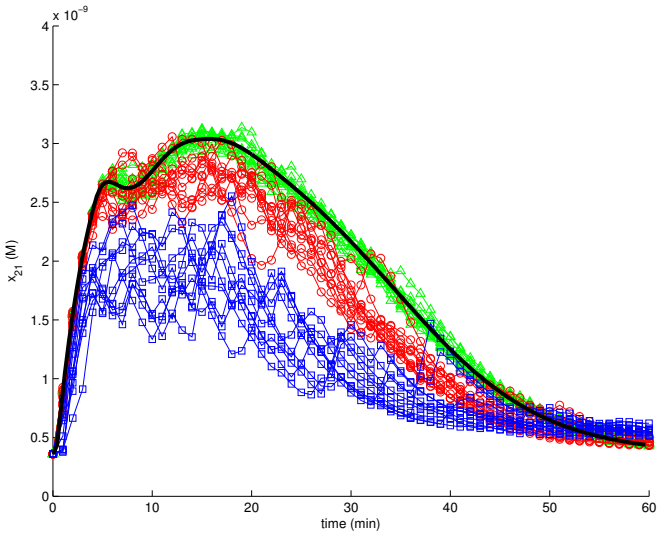

Fig. 2. Effect of changing system volume on x_{21} (surface GLUT4) from 0.93 nL (red circles) to 0.093 nL (blue squares) and to 9.3 nL (green triangles). The deterministic result is in black.

4.1 Methods

A stochastic model was derived from the Sedaghat model with feedback by assuming the differential equations could be represented explicitly as elementary reactions. A nominal system volume of 0.93 nL, the size of a typical human adipocyte, was chosen (Leonhardt et al. [1972]). Using the system volume, initial concentrations were converted to species populations. For variables in the deterministic model that had units of percentage (e.g. x_{21} is the percentage of total GLUT4 at the cell surface), estimates of concentrations for these variables were taken from the literature and used to calculate these chemical species' initial populations (Giri et al. [2004]).

Deterministic kinetic parameters were converted to the appropriate stochastic forms, and kinetic parameters that were functions of state variables in the Sedaghat model were included in StochKit by adding custom code to the propensity functions. Additional custom code was written to simulate the 15-minute pulse of insulin input and the explicit time delay that appear in the Sedaghat model (Sedaghat et al. [2002]).

Two sets of perturbation simulations were then done on the stochastic model to study the sensitivity of fluctuation magnitude. One set of simulations involved varying the system volume up and down 10-fold to study the effect of cell volume. In the other set of simulations, "sensitive" and "insensitive" reaction rates from the deterministic model (k_{-9} and k_{-1} respectively) were increased and decreased by 50%, holding volume constant, to give us a qualitative feel for the effect of these parameter perturbations on the stochastic model.

4.2 Results and analysis

As seen in Fig. 2, the stochastic trajectories tend to peak below the deterministic model, especially at small volumes. This difference is primarily due to a variable in the Sedaghat model that describes the combined effect

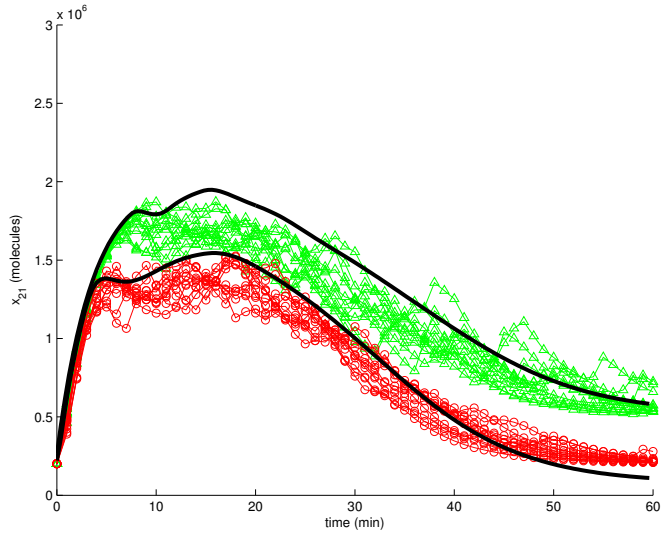

(a) x_{21} with k_{-9} perturbed down (green triangles) and up (red circles)

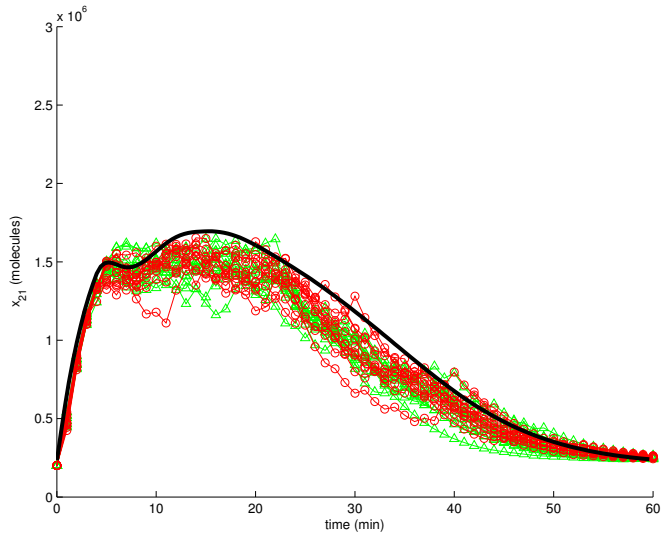

(b) x_{21} with k_{-1} perturbed down (green triangles) and up (red circles)

Fig. 3. Effect on x_{21} of perturbation of sensitive parameter (k_{-9}) versus that of insensitive parameter (k_{-1}) for the model without feedback

activated Akt and PKCζ have on the GLUT4 translocation rate to the cell surface – this "effect" has an upper bound in the model. Therefore, stochastic fluctuations in the amount of activated Akt and PKCζ near their peak values that would ordinarily raise the "effect" variable above the upper bound are capped while fluctuations below the deterministic values lead to lower surface GLUT4 (x_{21}) translocation propensities and lower surface GLUT4 values at peak stimulation.

Another observation to be made from Fig. 2 is that the stochastic model trends slightly above the deterministic model near the end of the numerical experiments (at approximately 50 minutes). This is primarily due to stochastic fluctuations in x_{13} around the deterministic steady-state value of 0.31% (See Appendix A.1). In the Sedaghat model, kinetic parameters k_{11} and k_{12} depend on state x_{13} and values of x_{13} below 0.31% lead to negative values for these parameters. This results in negative propensities in the SSA for reactions involving those parameters; negative propensities were capped at zero. Therefore, fluctuations in x_{13} below 0.31% have minimal downstream effects while fluctuations above 0.31% lead to increased x_{17}, x_{19} and, ultimately, larger values of x_{21} than the ODE model. This difference becomes negligible when the system volume is increased.

The magnitude of fluctuations in x_{21} (surface GLUT4) increased from ≈10% to ≈25% when the volume was decreased 10-fold and reduced to ≈5% when volume was increased 10-fold. As seen in Fig. 3, a 50% change in k_{-1}, an insensitive parameter, resulted in negligible change in peak value or relative fluctuation magnitude, while a 50% change in k_{-9}, a sensitive parameter, caused a ≈20% change in x_{21} peak value, with negligible effect on relative fluctuation magnitude. By comparing the two sets of stochastic experiments, we can argue that relative fluctuation magnitude depends primarily on volume and remains largely independent of parameter values, while peak values depend both on volume and the values of sensitive parameters.

5. CONCLUSION

In this paper, sensitivity analysis was used to minimize error in parameter estimation by optimization of input perturbation selection as well as state measurement selection. With model parameters gleaned from analysis of dynamic sensitivity, steady-state sensitivity analysis revealed a number of sensitive parameters suitable for drug targeting; also, we found that the addition of feedback mechanisms significantly changes the sensitivities with respect to a number of parameters. Finally, we used stochastic modeling to determine that system volume and parameter perturbations may have effects on the response of GLUT4 to insulin that are not captured by a deterministic model.

A number of criticisms can be leveled at this work; one possibility is that, although a number of parameters were removed due to *a priori* unidentifiability, more model parameter reduction possibly could have been done, as only 68% of the parameters were identifiable. Other possible criticisms include the fact that realistic state measurement data does not tend to be as continuous or as accurate as this analysis assumes (0.001 min per data point with 1% measurement error). More realistic numbers of time points and larger state measurement errors would likely result in fewer identifiable parameters with larger estimated variances. In addition, numerical inversion of a nearly singular FIM was needed to calculate estimated parameter variances which could have led to numerical errors.

Further work should include model validation, using the input and measurement selection developed here to determine parameters more closely and/or invalidate the model. A more comprehensive search on input perturbations and measurement selection may yield better results for parameter estimation. Incorporating expected fluctuation magnitude from our stochastic experiments into our input and measurement selections may result in a more realistic set of parameters identifiable from experiment.

In the course of developing this sensitivity analysis and the stochastic realization of the Sedaghat model, we found a number of shortcomings in the Sedaghat model. While portions of the model follow standard mass-action kinetics, we found a number of places in which the model was not mechanistically detailed. This led to a number of difficulties in our work – primarily in our stochastic simulations. We believe that further development of a more detailed model will be important to our understanding of insulin signaling. Incorporating recently discovered signaling components, such as those discussed by Schmelzle et al. [2006] and by Saltiel and Pessin [2003] may be useful.

Lastly, because insulin affects a number of other cellular processes, the integration of crosstalk (Sesti [2006]) or models that incorporate organism-level detail (e.g. pancreatic β-cell secretion of insulin) (Bertuzzi et al. [2007], Topp et al. [2000]) would yield a more complete understanding of the role of the insulin signaling cascade on glucose disposal and insulin resistance.

ACKNOWLEDGEMENTS

E. Kwei would like to acknowledge helpful discussion with S. R. Taylor and S. P. Hildebrandt.

REFERENCES

A. Bertuzzi, S. Salinari, and G. Mingrone. Insulin granule trafficking in beta-cells: mathematical model of glucose-induced insulin secretion. *Am J Physiol Endocrinol Metab*, 293(1):E396–409, 2007.

D. T. Gillespie. General method for numerically simulating stochastic time evolution of coupled chemical-reactions. *Journal of Computational Physics*, 22(4):403–434, 1976.

L. Giri, V. K. Mutalik, and K. V. Venkatesh. A steady state analysis indicates that negative feedback regulation of PTP1B by Akt elicits bistability in insulin-stimulated GLUT4 translocation. *Theoretical Biology and Medical Modeling*, 1:2, 2004.

H. Kitano, K. Oda, T. Kimura, Y. Matsuoka, M. Csete, J. Doyle, and M. Muramatsu. Metabolic syndrome and robustness tradeoffs. *Diabetes*, 53:S6–S15, 2004.

W. Leonhardt, H. Schneide, H. Haller, and M. Hanefeld. Human adipocyte volumes - maximum size, and correlation to weight index in maturity onset diabetes. *Diabetologia*, 8(4):287–291, 1972.

M. J. Quon. Advances in kinetic analysis of insulin-stimulated GLUT-4 translocation in adipose cells. *American Journal of Physiology*, 266(1):E144–E150, 1994.

A. R. Saltiel and J. E. Pessin. Insulin signaling in microdomains of the plasma membrane. *Traffic*, 4(11): 711–716, 2003.

K. Schmelzle, S. Kane, S. Gridley, G. E. Lienhard, and F. M. White. Temporal dynamics of tyrosine phosphorylation in insulin signaling. *Diabetes*, 55(8):2171–2179, 2006.

A. R. Sedaghat, A. Sherman, and M. J. Quon. A mathematical model of metabolic insulin signaling pathways. *American Journal of Physiology-Endocrinology and Metabolism*, 283(5):E1084–E1101, 2002.

G. Sesti. Pathophysiology of insulin resistance. *Best Practice and Research Clinical Endocrinology and Metabolism*, 20(4):665–679, 2006.

S.R. Taylor, R. Gunawan, K. Gadkar, and F. J. Doyle III. BioSens sensitivity analysis toolkit v2β. `http://www.chemengr.ucsb.edu/~ceweb/faculty/doyle/biosens/BioSens.htm`, 2005.

B. Topp, K. Promislow, G. de Vries, R. M. Miura, and D. T. Finegood. A model of beta-cell mass, insulin, and glucose kinetics: Pathways to diabetes. *Journal of Theoretical Biology*, 206(4):605–619, 2000.

S. Wanant and M. J. Quon. Insulin receptor binding kinetics: Modeling and simulation studies. *Journal of Theoretical Biology*, 205(3):355–364, 2000.

D. E. Zak, G. E. Gonye, J. S. Schwaber, and F. J. Doyle. Importance of input perturbations and stochastic gene expression in the reverse engineering of genetic regulatory networks: Insights from an identifiability analysis of an in silico network. *Genome Research*, 13(11):2396–2405, 2003.

Appendix A. ODE MODEL

A.1 State variables

The states mentioned in Fig. 1 and in the text are summarized below.

State	Description
x_1	Insulin input (M)
x_2	Unphosphorylated, unbound surface receptors (M)
x_3	Unphosphorylated, once-bound surface receptor (M)
x_4	Phosphorylated, 2×-bound surface receptors (M)
x_5	Phosphorylated, 1×-bound surface receptors (M)
x_6	Unphosphorylated, unbound intracellular receptors (M)
x_7	Phosphorylated, 2×-bound intracellular receptors (M)
x_8	Phosphorylated, 1×-bound intracellular receptors (M)
x_9	Unphosphorylated IRS1 (M)
x_{10}	Tyrosine-phosphorylated IRS1 (M)
x_{10a}	Serine-phosphorylated IRS1 [feedback only] (M)
x_{11}	Unactivated PI3K (M)
x_{12}	Activated IRS1-PI3K complex (M)
x_{13}	$PI(3,4,5)P_3$ (% of total)
x_{14}	$PI(4,5)P_2$ (% of total)
x_{15}	$PI(3,4)P_2$ (% of total)
x_{16}	Unactivated Akt (% of total)
x_{17}	Activated Akt (% of total)
x_{18}	Unactivated PKCζ (% of total)
x_{19}	Activated PKCζ (% of total)
x_{20}	Intracellular GLUT4 (% of total)
x_{21}	Surface GLUT4 (% of total)

A.2 Model parameters

The model equations were taken from Sedaghat et al. [2002]. However, a number of parameters, listed below, had to be changed for purposes of sensitivity analysis.

$$k_{-3} = 0.2\, min^{-1} PTP$$

$$k_6 = 0.461\, min^{-1} PTP$$

$$k_7 = 4.64 \times 10^{12}\, min^{-1}$$

$$k_{-7} = 1.396\, min^{-1} PTP$$

$$k_{7'} = \begin{cases} \dfrac{6.93\, min^{-1} \left[x_{19}\left(t-\tau\right)\right]^4}{K_d^4 + \left[x_{19}\left(t-\tau\right)\right]^4}, \text{for feedback} \\ 0, \text{for no feedback} \end{cases}$$

$$k_{13} = 0.0115\left(0.2x_{17} + 0.8x_{19}\right) + 6.96 \times 10^{-3}\, min^{-1}$$